ISSN 0001-4338, Izvestiya, Atmospheric and Oceanic Physics, 2024, Vol. 60, No. 4, pp. 448–462. © Pleiades Publishing, Ltd., 2024.

Methane Emissions and Hydrological Structure of the Zeya Reservoir (Russia) in the Warm Period

P. N. Terskii[a, e, *], S. L. Gorin[a, d], I. A. Repina[a, b], S. A. Agafonova[a, c], M. V. Zimin[c], V. P. Shesterkin[f], and F. A. Shchekotikhin[c]

[a] *Obukhov Institute of Atmospheric Physics, Russian Academy of Sciences, Moscow, 119017 Russia*
[b] *Research Computing Center, Moscow State University, Moscow, 119234 Russia*
[c] *Faculty of Geography, Moscow State University, Moscow, 119991 Russia*
[d] *Russian Federal Research Institute of Fisheries and Oceanography, Moscow, 105187 Russia*
[e] *Water Problems Institute, Russian Academy of Sciences, Moscow, 119333 Russia*
[f] *Institute of Water and Ecology Problems, Far Eastern Branch, Russian Academy of Sciences, Khabarovsk, Khabarovsk krai, 680000 Russia*
**e-mail: pavel_tersky@mail.ru*

Received February 18, 2023; revised April 16, 2024; accepted May 29, 2024

Abstract—Based on the results of field measurements of methane concentrations in water and its specific fluxes from the water surface, the emission of methane in the warm season from the Zeya Reservoir, one of the largest artificial hydropower facilities in Russia, has been assessed for the first time. Data were obtained during field surveys carried out in September 2021 and July 2022. Hydrological and hydrochemical surveys have made it possible to obtain information about the thermal, oxygen, and chemical structure of the reservoir water column, as well as carry out a comprehensive zoning of its water area. A digital model of the relief of the Zeya reservoir bed is developed, which, together with zoning, has made it possible to perform detailed calculations of the total methane emission from the Zeya Reservoir. It has been found that, for the reservoir, the main sources of organic matter and methane are swampy tributaries and runoff of organic matter from the shores, which enters the water area coastal areas. These areas accumulate allochthonous organic matter and are characterized by high methane fluxes. The total CH_4 flux from the Zeya Reservoir surface is significantly higher in summer (when maximum heating of shallow waters is observed) than in the autumn. The CH_4 emission coefficients obtained by the authors from the Zeya Reservoir (8.6–17.2 kgCH_4/ha) correspond to the coefficients presented in the Supplements to the 2019 IPCC Guidelines for Boreal Reservoirs.

Keywords: greenhouse gas emissions, methane, hydrological structure, hydrological regime, water temperature, Zeya Reservoir, field survey, digital elevation model

DOI: 10.1134/S0001433824700373

INTRODUCTION

In 2021, the Obukhov Institute of Atmospheric Physics, Russian Academy of Sciences, commissioned by PAO RusHydro, began a 3-year cycle of research on the topic “Measuring greenhouse gas emissions and assessing the absorption capacity of hydropower facilities.” This project is based on in situ measurements of the balance of greenhouse gases, primarily methane (CH_4), at large reservoirs in Russia (Repina et al., 2022). In addition to its fundamental importance, the problem of assessing greenhouse gas (GHG) emissions also has a practical aspect, which is especially important for Russia: currently there is no certainty regarding the carbon neutrality of domestic hydroelectric power plants that use water resources from reservoirs to generate electricity.

The emission of GHGs (and primarily methane) from the surface of reservoirs occurs throughout their entire life. However, the maximum flow values are observed in the first years of filling. Over time, emissions decrease, but in some cases, a decrease in carbon activity not only does not occur, but even an increase in emissions is recorded (Elistratov et al., 2014). At low temperatures, methane is resistant to oxygen; in general, it is chemically neutral and is not absorbed by alkalis and weak acids (Garkusha and Fedorov, 2021).

An inventory of global data on methane emissions from the surface of reservoirs, given in (Deemer et al., 2016) and refined in (Deemer and Holgerson, 2021; Rosentreter et al., 2021), showed that CH_4 emission significantly depends on the climatic zone, flow, and age of the reservoir and can vary greatly even within the same climatic zone.

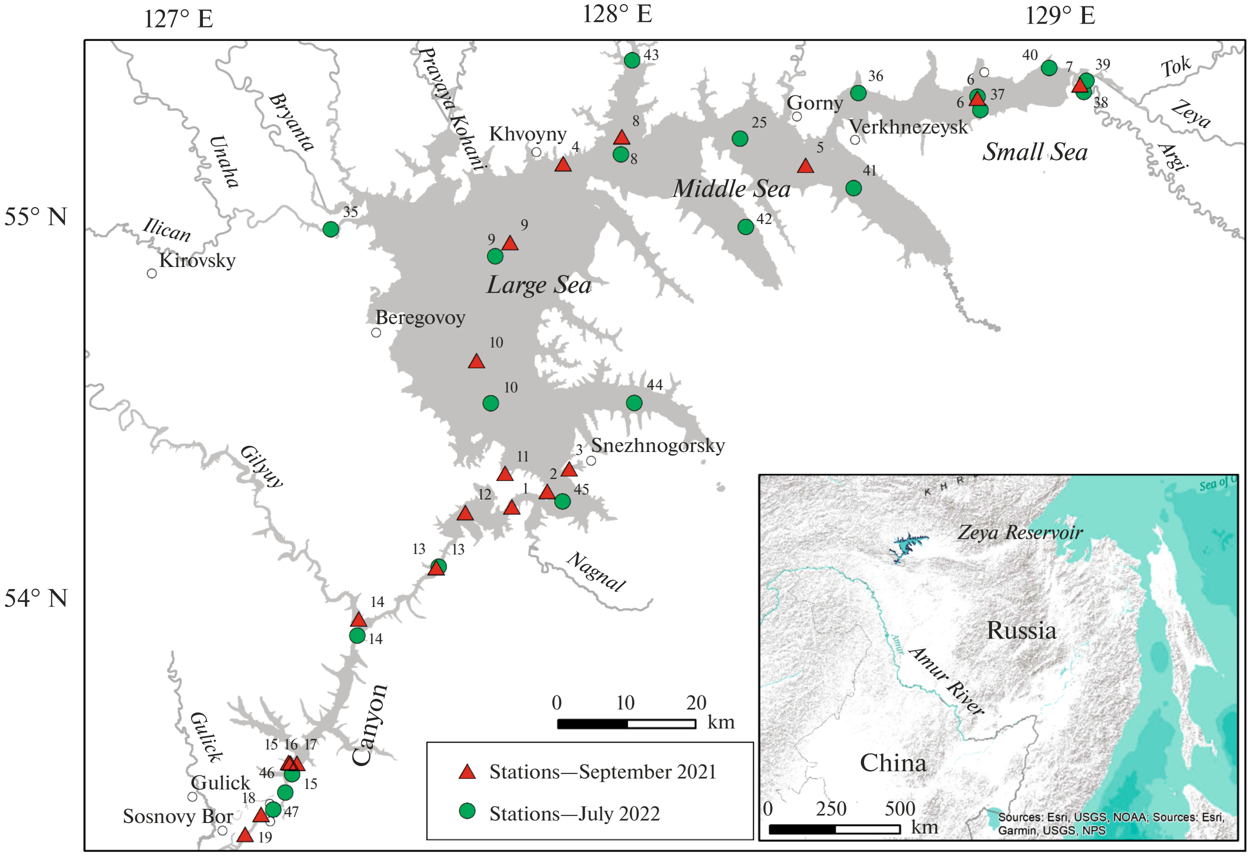

Fig. 1. Map of the Zeya Reservoir with the location of field work stations in 2021 and 2022. Note: continuous numbering is provided for the entire series of expeditions; stations with the same number characterize the same homogeneous area of reservoir.

GHG fluxes from reservoirs often exhibit diurnal and synoptic variability—on time scales ranging from minutes to hours and even during individual day and night cycles (Sieczko et al., 2020; Grechushnikova et al., 2019). The variability of these flows on a seasonal scale is also high, depending on the activity of production and destruction processes, river inflow, fluctuations in reservoir levels, and the mixing layer size and dynamics (Deemer et al., 2016; Grechushnikova et al., 2018, 2019).

Field research by the team of authors on the Zeya Reservoir has an expeditionary format, in which measurements are taken over the entire reservoir area for several days twice a year. Therefore, this work does not take into account the CH_4 flux variability on time scales less than a season (for example, diurnal and synoptic).

The purpose of this article is to provide a quantitative description of hydrological conditions as the basis for the formation of CH_4 emission in the Zeya Reservoir water column during the warm period, show their relationship with CH_4 flows in relatively high- and low-water conditions, and assess the total CH_4 emission from the reservoir.

STUDY AREA

Zeya Reservoir is one of nine reservoirs being studied by the authors of the project. It has the characteristic features of temperate zone reservoirs. However, it is also characterized by unique features, due to a combination of morphological features (a vast part with depths of up to 50 m and a canyonlike part with depths of up to 100 m), significant area and volume, high flow, and pronounced seasonality in the hydrological regime.

Zeya Reservoir is located in the Far East of Russia on the southern slopes of the Stanovoy Range. It was formed in the middle reaches of the Zeya River— the largest tributary of the Amur River. In addition to the main river, large watercourses such as Gilyuy, Bryanta, and Unakha flow into the reservoir. For the convenience of planning work and describing the results, we have identified characteristic areas of the water area, which are called the Small Sea, Middle Sea, Large Sea, and Canyon (Fig. 1).

Filling of the Zeya Reservoir bowl began in 1974, and the reservoir was filled to the normal headwater level (NHL) in 1985 (*Skhema*..., 2010). The main characteristics of the reservoir are given in Table 1.

Table 1. Zeya Reservoir main characteristics

Characteristic	Value	Data source
Water level: UMO/NPU/FPU*, m abs.	299.0/315.0/322.0	(Rules..., 2018)
Length: at UMO and NPU, km	225 and 290	Own calculations
Width: greatest (average) at NPU, km	24 (8.4)	(*Skhema*..., 2010)
Depth: greatest (average**) at NPU, m	96 (28.7)	Own assessments
Area: at UMO/NPU/FPU, km^2	1620/2419/2955	(Rules..., 2018)
Volume: at UMO/NPU/FPU/ average annual, km^3	36.3/68.4/87.4/63.0	(Rules..., 2018)
Catchment area, km^2	83 800	(Rules..., 2018)
Average annual water inflow, taking into account sediments in the water area, km^3	25.2	(Rules..., 2018)***
Average annual flow at the dam site, km^3	24.8	(Rules..., 2018)***
Evaporation from the water area of the reservoir, km^3	0.38	(Rules..., 2018)***
Water exchange coefficient****	0.39	Own calculations

* UMO, dead storage level; NPU, normal headwater level; and FPU, forced headwater level.
** Average depth at NPU, quotient of dividing the volume by the area at NPU.
*** Estimated values for 1901–2017.
**** Water exchange coefficient, quotient of dividing the flow at the dam site by the long-term average volume of reservoir.

According to the Zeya hydroelectric power station operational data (http://www.rushydro.ru), the average long-term water level for the period 2005–2021 is 312.6 m abs. The minimum level is observed in March to April—about 309–310 m abs; in some years it drops to 307 m abs. The maximum level is 316–318 m abs, typical for the summer–autumn period; in some years (2007, 2013, and 2021) the level can exceed 318 m abs.

The water regime of the Zeya Reservoir is determined mainly by the Zeya River and its largest tributary—the Gilyuy River. Based on the nature of the intra-annual flow distribution, these rivers belong to the Far Eastern type of water regime, which is characterized by high water content in the warm part of a year: spring–summer floods, turning into high floods in the second half of summer and early autumn. Often, rain floods are larger in magnitude (maximum water flow and runoff volume) than floods. In winter, river flow is minimal. In a year with average water content, from May to August, ~56% of the annual volume of water enters the reservoir, in September and October ~41%, and the winter months account for only ~3%. For an average year in terms of water content, the share of rain recharge exceeds 70%, snow recharge reaches 25%, and groundwater reaches 5% (Rules..., 2018). In a long-term plan, the river water average annual influx into the reservoir varies from 431 to 1220 m^3/s (in a very low-water and very high-water years, respectively) (Rules..., 2018).

According to the chemical composition, the waters of Zeya Reservoir are ultrafresh waters of the hydrocarbonate class of calcium group (Shesterkin et al., 2016). The high swampiness of the Zeya Reservoir basin distinguishes it from the reservoirs of the Far East and Siberia due to its high content of organic matter (Arefina et al., 2010).

In the Zeya Reservoir area, the climate is ultracontinental with monsoonal features, and winters are severe, with little snow; summers are moderately cool (in the north) and warm (in the south). The air temperature is –4.6°C on average for the year, –31.0°C on average for January, and 18.0°C on average for July according to the Bomnak weather station (WMO code 31253). The air temperature passes through 0°C in mid-April and mid-October. During the warm period, there is a large amount of precipitation, and heavy rainfall is possible. Average annual precipitation is ~573 mm, of which ~85% falls from mid-April to mid-October (http://aisori-m.meteo.ru).

In the Zeya Reservoir basin, coniferous taiga and forest-tundra, permafrost, and swamps are common. On the reservoir banks there are six settlements with a population of about 4500 people; in the lower pool there is the city of Zeya with a population of 22000 people (*Skhema*..., 2010).

Characteristics of Working Conditions

Expedition studies on the Zeya Reservoir were carried out from September 17 to 23, 2021, and from July 25 to 31, 2022. Hydrological conditions of work in 2021 and 2022 differed significantly (Table 2). In 2021, the work was carried out during the summer–autumn flood period. During the warm period (May to early

Table 2. Hydrological conditions during the period of work on the Zeya Reservoir in 2021 and 2022

Expedition period	September 17–23, 2021	July 26–31, 2022
Water level (WL), m abs.	318.01–317.89	311.65–311.69
WL long-term average for 2005–2020 calendar period of the expedition, m abs.	314.90–315.04	312.65–313.38
Total flow rate, m^3/s	3360–3276	713–726
Flow through the spillway, m^3/s	2517–2238	0
Reservoir volume, km^3	75.34–76.10	60.68–60.77
Volume of inflow at the start of work (from April 20), km^3	42.0	10.5
Discharge of water through the HPP before operation (from April 20), km^3	23.4	6.3
Accumulation of inflow into the reservoir before operation (from April 20), km^3	18.6	4.2
Discharge through the surface spillway before operation (from April 20), km^3	8.6	0.0

Table 3. Types and volume of field work in the Zeya Reservoir in 2021 and 2022

Types of research		Work period	
		September 2021	July 2022
Measuring hydrological characteristics (sounding)	Stations	19	21
Water sampling for CH_4	Stations	18	21
	Total samples*	80	150
CH_4 flux measurements	Stations	14	17
	Total samples**	116	127
Water sampling for chemical composition	Stations	10	14
	Total samples	20	25

* Including replicates and ** including atmospheric air samples (1 sample per station).

September), abnormally high amounts of precipitation were observed (up to 850 mm), and the daily amount was 50 mm. The weather directly during the work period was clear, without precipitation; air temperature varied from –2 to +21°C, water temperature on the surface from +9.6 to +15.1°C (in the lower pool +8.4°C), and wind during the work period was variable up to 6 m/s. The evacuation of the reservoir was done through turbines and surface spillways.

The expeditionary investigation period in 2022 corresponded to the stage of the beginning of reservoir summer filling (the beginning of the flood period). The weather in the first part of this period was characterized by anticyclonic type and, in the second part, by frontal precipitation. Air temperature was from +15.2 to +27.8°C; water temperature on the surface was from +11.6 to +26.7°C (in the lower pool +4.7°C). The wind during the work period, as in 2021, was variable, up to 6 m/s. The water level was 3.4 m below the NHL; evacuation of reservoir was done only through turbines.

MATERIALS AND METHODS

Field Work Methods

Expeditionary studies at the Zeya Reservoir included measurements of hydrological characteristics of water (temperature, electrical conductivity, and dissolved oxygen content), water and air sampling to determine CH_4 concentrations and the magnitude of its flux at the water/atmosphere interface, and water sampling for chemical composition (major ions, pH, mineralization, total iron, and silicon). The spatial arrangement of observation stations is shown in Fig. 1; information on the scope of work is given in Table 3. All work was carried out from on board the boat. In most cases, anchoring the vessel was impossible due to the great depths and the clutter of the bottom with woody debris, so the measurements were carried out while drifting.

Hydrological characteristics were measured using a YSI 6600 probe at all stations (water sampling for chemical composition was not carried out at all stations). The accuracy of water temperature measurements was 0.05°C; electrical conductivity was ~3–5 μS/cm. The conversion of electrical conductivity to salinity was carried out to determine the salinity of water at all stations using the coupling equation obtained based on the data of measuring salinity in individual water samples under laboratory conditions. Oxygen content was measured by a membrane sensor. Its accuracy is low, so the results of these measurements should not be considered in strictly quantitative terms; within the framework of the current work, it was enough to interpret them at a qualitative level (there is a deficiency/no deficiency of oxygen). The resolution of sounding in depth ranged from 1 to 5 m, depending on the total depth at the station and the nature of observed changes in hydrological characteristics.

Water samples for CH_4 and chemical composition were taken with a 2-L Niskin system bathometer with a marked cable (cable length 100 m). Samples for CH_4 concentration were taken in duplicate in 20 mL bottles. Sampling horizons were assigned: in the fall of 2021 in the surface layer, under the layer of water temperature jump and in the bottom layer; in the summer of 2022 in the surface layer, under the photic layer (5 m), above and below the temperature jump layer (15 and 30 m, respectively), as well as in the bottom layer (1 m above the bottom). At some stations, additional horizons were assigned (for example, in areas with upwelling, or near large tributaries).

Measurements of CH_4 fluxes were carried out using the floating chamber method (two plastic chambers, volume 7–10 L). Characteristics of the chambers comply with the UNESCO methodology for measuring CH_4 emissions from water bodies. Exposure time (1 h) was divided into two series of 30–40 min each. The pumping of air in the tube going from the chamber to the sampler syringe, by 2 syringe volumes (60 mL capacity), was performed before each sampling.

Water samples for chemical composition were taken in 1.5 L containers made of chemically inactive plastic and stored at a temperature from +8 to +15°C for 3–8 days before entering the laboratory. In these samples, the main ions were determined and water mineralization was calculated from them. Then, based on the data, a relationship was built between salinity and the measured electrical conductivity of water. In all cases, the relationship is similar, very close to linear (correlation coefficient 0.95–0.98). Sampling locations and horizons were assigned in such a way that the result covered the entire range of salinity expected in the reservoir according to the literature.

Weather observations were carried out using a Kestrel 5000 portable weather station at each station at the beginning of sampling cycle and included measurements of air temperature and humidity, wind speed, and atmospheric pressure.

Depths at the stations were measured using an echo sounder. Locations of stations were determined using a portable GPS receiver in the WGS-84 coordinate system.

Methods of Laboratory and Office Working

The chemical composition of waters of the Zeya Reservoir was determined at the Institute of Water and Environmental Problems, Far Eastern Branch, Russian Academy of Sciences, according to the methods described in the regulatory documents (Regulatory document..., 2009). The content of sodium and potassium ions was determined on a flame photometer; calcium and magnesium ions, hydrocarbonate, and chloride ions by titration; sulfate ions on a photometer by the turbidimetric method; and water color on a photocolorimeter.

The CH_4 concentration in samples of air and water extract was determined in the laboratory of the Obukhov Institute of Atmospheric Physics, Russian Academy of Sciences, using the headspace method (Bastviken et.al., 2010) on a gas chromatograph with a Khromatek-Kristall 5000.2 flame ionization detector according to (RD 52.44.816¬2015).

The emission of CH_4 as a result of the degassing of water during its discharge through the Zeya hydroelectric complex was estimated as the product of water flow and the difference in the CH_4 concentration in the water between the upper and lower pools (taking into account the concentration of CH_4 in the air).

Methodology for Calculating Total Methane Emissions

The calculation of the total CH_4 emission from the Zeya Reservoir surface is based on the results of field measurements of specific CH_4 fluxes and their subsequent averaging for the selected areas (see section Results) taking into account the areas occupied by shallow waters. For this purpose, the authors built a digital model of Zeya Reservoir bed relief. Sources of topographic information for this model were topographic maps at a scale of 1 : 100000, which show elevation points and isohypses in the Zeya River valley before flooding and isobaths during the period of incomplete filling in the late 1970s; satellite images of Landsat and Sentinel-2 (with a spatial resolution of selected channels of 15 and 10 m, respectively) for the period of 2013–2020, on which the contours of the reservoirs water area are read at different levels of its filling (306–319 m abs.); and data from field measurements of reservoir depths. A digital relief model in absolute elevations was built by the Hutchinson method (Topo to Raster method) using the ESRI ARCGIS GIS package with a spatial resolution of 25 m.

To move from spatially discrete measurements at stations to estimates of total emissions, the entire reservoir was divided into areas identified within the framework of this study (see Results). Based on the density of stations, the number of horizons sampled, the relationship of CH_4 fluxes with depth, and the actual spatial distribution of specific CH_4 fluxes, deep zones were expertly identified within morphological regions. This was done to calculate the total methane emissions as accurately as possible, namely, in order to divide stations into shallow and deep-water, and then calculate average methane fluxes within these zones based on observational data at the corresponding stations (assigned to the deep- and shallow-water zones). In the summer of 2022, zones with a depth of less than 30 m were identified in the Large and Middle Seas, within which specific CH_4 fluxes were significantly higher than in the rest of water area. Local maxima of CH_4 fluxes (so-called "hot spots" (Darling and Gooddy, 2006)), which were discovered during the autumn expedition of 2021 in the upper part of the Canyon, were separately taken into account.

Total CH_4 emissions are given in range form. The lower "rough" estimate consisted of averaging the specific fluxes over all stations within each region. The total CH_4 emission from the entire reservoir was determined by summing the emissions, which were obtained by multiplying the average specific CH_4 flux calculated for each region by the area of the corresponding regions. The upper "detailed" estimate of the total CH_4 emission was carried out taking into account areas of the water area with a depth of less than 30 m, based on the shares of the areas of regions occupied by these sites. Emissions from hot spot areas were assessed by an expert assessment of the area of shallow bays described by hot spots (at the level of 3 and 5% of the area for the lower and upper estimates, respectively). Both estimates also include the CH_4 flux resulting from degassing of water when it is discharged through the Zeya hydroelectric power station dam.

Growing season in the Zeya Nature Reserve (Russia) area is 130–140 days (http://oopt.info/zeysky/physgeo.html). To calculate the CH_4 emission coefficient, an average value of 135 days was taken. It should be noted that, in 2021, the measurements were taken at the end of the growing season and, in 2022, closer to its middle, so the results do not fully describe the entire growing season.

Methodology for Calculating Methane Reserves in a Water Body

To estimate CH_4 reserves in a reservoir, the averaging of its concentrations was used by nonlinear automated interpolation over the volume of the reservoir for each grid node by taking into account the values of the surrounding station points. Using the digital relief model obtained in this work, in each layer of reservoir with a step of 2 m in depth, the methane concentration values were interpolated over the layer area using the inverse cost weighting (ICW) method (Wing et al., 2004). This method is a derivative of the standard inverse distance weighted (IDW) method, but allows one to correctly take into account natural barriers (such as capes and peninsulas, that is, station points may not be in direct visibility from each other). As a result, the verticals with a layer-by-layer distribution of methane concentration were obtained for each season. Then, the volume-weighted average stock of methane in the reservoir was obtained as the sum of layer-by-layer products of methane concentration and the volume of each layer.

RESULTS

Reservoir Hydrological Structure in 2021 and 2022

During the expedition in September 2021, the reservoir temperature stratification and the temperature jump layer (TJL) were well expressed, especially in the Large Sea and in the Canyon, that is, where there are great depths. TJL lay at depths below 20–30 m and, in general, became deeper as it approached the dam. The TJL depth varied from 15–20 m in the north (in the area of station 6) to 30–40 m in the south of the Large Sea and up to 60 m at the dam in the area of stations 15–16 (Fig. 2a). The average weighted water temperature along the profile was 9.4°C. The lowest temperatures at the bottom (4.9–5.5°C) were observed in the center of the Large Sea (stations 9–10), and the highest were in the Middle Sea (7–9°C) (stations 5 and 25) and Canyon (6–7°C) (stations 13–16). The reservoir was saturated with oxygen throughout its entire depth; no zones of anoxia were identified. The weighted average saturation value along the longitudinal profile was 74%. The least oxygenated zones were identified in the region of greatest depths in the Canyon, while the saturation value exceeded 50% (Fig. 2b). The profile-weighted average mineralization value was 22.3 mg/dm^3. The highest mineralization of water was observed in the Zeya River (36.1 mg/dm^3), below Bomnak mineralization varied within 26–29 mg/dm^3 (station 6). Mineralization slightly increased with depth (Fig. 2c).

In 2022, during the expedition (July 26–31), the reservoir temperature stratification was also well expressed; the TJL was located at depths of 15–20 m and occupied a relatively constant position. The average weighted water temperature along the profile was 8.5°C. The lowest temperatures were at the bottom (3.9–4.1°C) in the Large Sea and Canyon (stations 9, 10, 13–16) and the highest (up to 5°C) in the Small and Middle Seas (stations 25, 36, 37, and 41), in bays and rivers. At the surface, the water temperature reached 26°C (see Fig. 2a). Also, the temperature was high in the Zeya River and Argi River during the rain flood—up to 23°C. The reservoir water column was saturated with oxygen throughout its entire depth; no zones of anoxia were identified. The weighted average value of O_2 saturation along the longitudinal profile was 71%. The least O_2-saturated zones were identified in the area of greatest depths in the Canyon, as well as

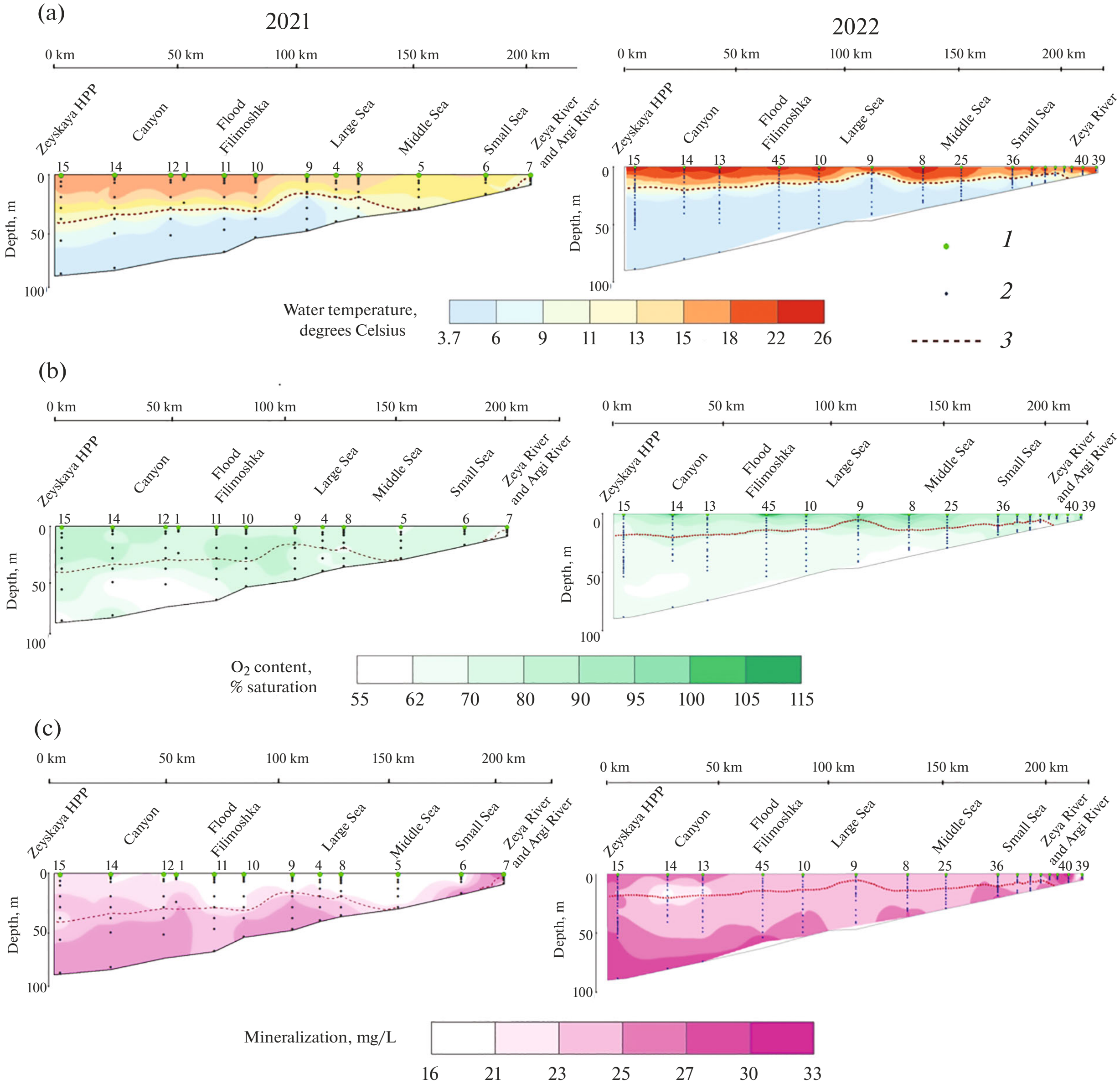

Fig. 2. Distribution of water temperature (a), dissolved oxygen content (b), and salinity (c) along the longitudinal profile of Zeya Reservoir according to expeditionary data in September 2021 (left) and July 2022 (right). Designations: (*1*) stations and their numbers, (*2*) vertical measurement points, and (*3*) temperature jump layer.

in the Middle Sea in the bottom layer, with saturation values exceeding 55%. The maximum concentration of dissolved oxygen (up to 115% saturation) was recorded in the surface layer of water in the Large Sea (stations 9 and 10) (see Fig. 2b); the minimum was in the bottom layer of water in the Small Sea (stations 7 and 37) (about 50%). At the beginning of the rain flood, the Argi River was saturated with oxygen up to 100%, which may be due to both the entry of aerated rainwater directly into the watercourse and the photosynthetic activity of phytoplankton in the river waters. The maximum values of mineralization, as before, were noted in the water of the mouths of the Zeya and Argi rivers (32.7 and 42.8 mg/dm^3). Also, high mineralization was observed in the bottom layer in the Canyon (up to 30–33 mg/dm^3) and throughout the entire water column in the Small Sea (about 30 mg/dm^3) (see Fig. 2c). The lowest mineralization was observed at the Canyon border and the Large Sea, as well as in the Middle Sea (far from river mouths).

Methane Content in Water

In the fall of 2021, the weighted average concentration of CH_4 in water was 1.34 μL/L. Increased concentrations were observed in the Small Sea (station 6)

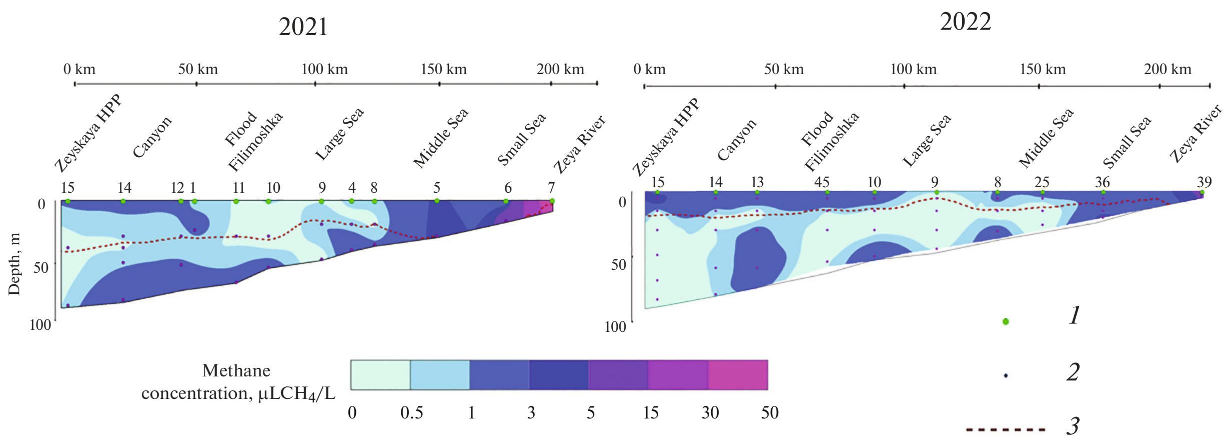

Fig. 3. CH_4 content in water along the longitudinal profile of Zeya Reservoir according to expeditionary data in September 2021 (left) and July 2022 (right). Designations: (*1*) stations and their numbers, (*2*) vertical measurement points, and (*3*) temperature jump layer.

(from 3–5 to 30 µL/L), especially in the zone of headwater wedging out—in the Argi River confluence zone (up to 49 µL/L). Reduced concentrations (less than 3 µL/L) were detected in Canyon (stations 13–16). The minimum concentrations of CH_4 in water were observed in the Large Sea (stations 9 and 10) and near the dam (stations 15–16) (less than 1 µL/L) (Fig. 3). In September 2021, in the upper reaches of the reservoir, CH_4 concentrations in water were an order of magnitude higher than in July 2022, when the river water inflow volume was significantly lower.

In summer 2022, the weighted average concentration of CH_4 in water was 1.01 µL/L. Its maximum concentrations are found in the Zeya and Argi rivers (5.3 and 12.5 µL/L, respectively). Increased values (up to 3–5 µL/L) were detected in the Small Sea upper part. Reduced CH_4 values (0.1–1.0 µL/L) are in the Canyon and in the center of the main water area (stations 9 and 10). Minimum concentrations of CH_4 (about 0.10–0.15 µL/L) were noted near the dam at depths of 30–70 m (see Fig. 3). In bays, in general, the concentration of CH_4 in water is higher than at deep stations.

In 2021, the methane reserve in the Zeya Reservoir water was significantly greater than in 2022. This difference in methane reserves was approximately proportional to the reservoir volume at the time of the work (Table 4).

Specific Flux from the Water Area and Methane Release during Degassing at the HPP Dam

During the period of expeditionary research in September 2021, CH_4 concentrations in the air above the reservoir water area varied between 1.8–2.8 ppm. In the open water area, the specific CH_4 flux varied in the range of 0.7–5.1 $mgCH_4/m^2/day$ (Fig. 4a). Significantly higher values of the specific CH_4 flux were detected at the mouth of the Argi River (36–57 $mgCH_4/m^2/day$) and in a shallow bay ("hot spot") on the border of the Large Sea and the Canyon (station 2) (31–246 $mgCH_4/m^2/day$). The large scatter in the specific flux values (by an order of magnitude) is probably associated with its intensive transport in gas bubbles released from bottom sediments.

During the study period in July 2022, CH_4 concentrations in the air were 2–3 ppm. Specific CH_4 flux varied within the range of 0.9–42 $mgCH_4/m^2/day$ with a separate outlier measured maximum of 137 $mgCH_4/m^2/day$ in the Unaha River (Fig. 4b). Compared to the fall of 2021, the methane flux values in the Large Sea did not differ significantly. In the Canyon in July 2022, the specific flux of CH_4 was 2–3 times higher (5–9 $mgCH_4/m^2/day$) than in 2021; in the Small Sea it was noticeably more. At the Argi River mouth in July 2022, specific methane flux values comparable to September 2021 were observed. Thanks

Table 4. Weighted average concentration and reserve of methane in the water of the Zeya Reservoir

Dates (expedition period)	Water level (WL), m abs.	Weighted average concentration of CH_4 in water, µL/L	Reservoir volume, km^3	CH_4 reserve, m^3
September 17–23, 2021	318.01–317.89	1.34	75.4	101 200
July 26–31, 2022	311.65–311.69	1.01	60.7	60 700

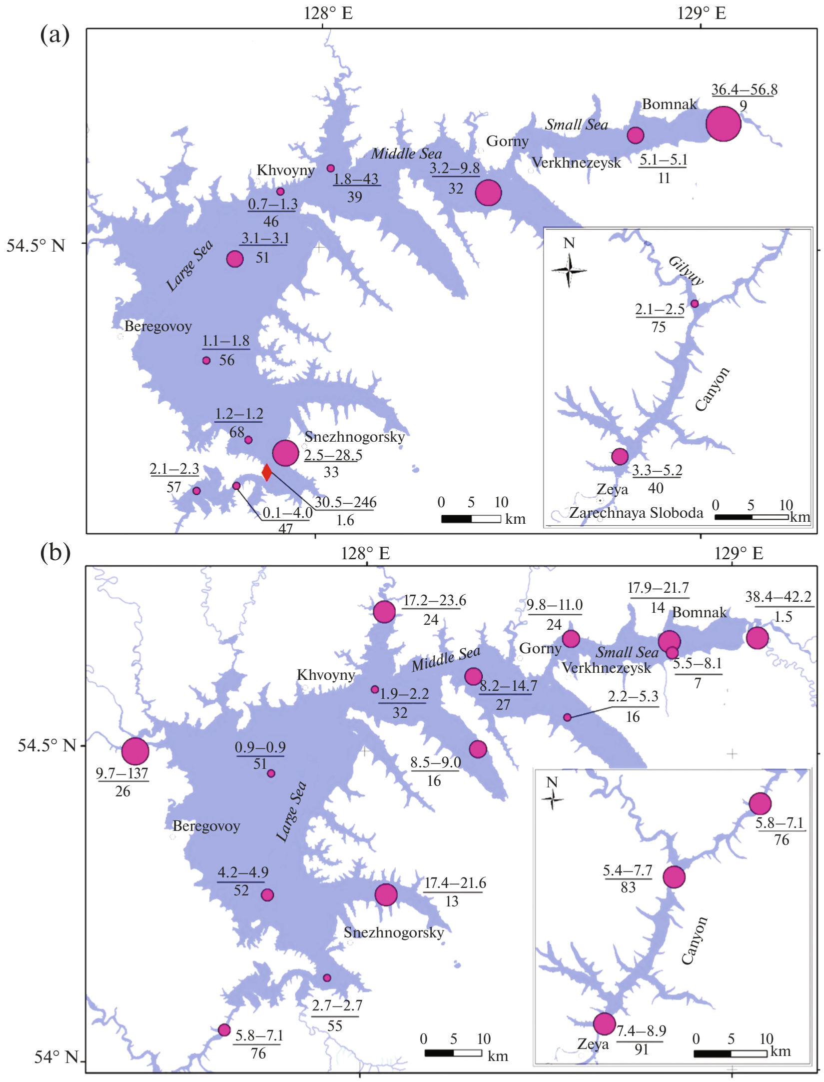

Fig. 4. Specific methane fluxes from the surface of Zeya Reservoir in September 2021 (a) and July 2022 (b). The numerator shows the range of measured flows (mgCH_4/m^2/day); the denominator shows the reservoir depth at the station (m). The red diamond indicates the location of the hot spot in 2021.

to the increase in the number of observation stations in the bays in 2022, additional information has been obtained on the spatial distribution of CH_4 specific flux values. Its maximum flows were detected at the Argi River mouth, in individual bays, and the Small Sea, and minimal ones were above the channel in the Large Sea and Canyon.

A general tendency for the feedback of CH_4 concentrations with the depth of stations was revealed. This relationship has a general form close to a power-law dependence (Fig. 5), but the closeness variability of this relationship over time is large (in 2021 the relationship was closer than in 2022). This relationship cannot be considered a calculated equation ($R^2 \sim 0.4$), but only as an illustration of the pattern and as a guide for identifying the conditions for the strongest uncertainty of this relationship. The greatest dispersion of CH_4 flux and concentrations is observed at station depths of 10–30 m. The most stable low fluxes are observed in areas with depths of more than 30 m.

In the fall of 2021, under operating conditions of the surface spillway, the emission of CH_4 during degassing amounted to 175 kgCH_4/day (less than 0.1% of the total emission). On the day of sampling in the hydroelectric power station upstream and downstream, the CH_4 content in the upstream at the turbine water intake horizon was 0.25 mg/m^3, at the spillway horizon 0.96 mg/m^3, and in the downstream 0.12 mg/m^3. The water flow through the turbines was 1038 m^3/s, and through the spillway 2238 m^3/s (http://www.rushydro.ru/).

During the warm period of 2022, the surface spillway at the dam was not used—there was no need for

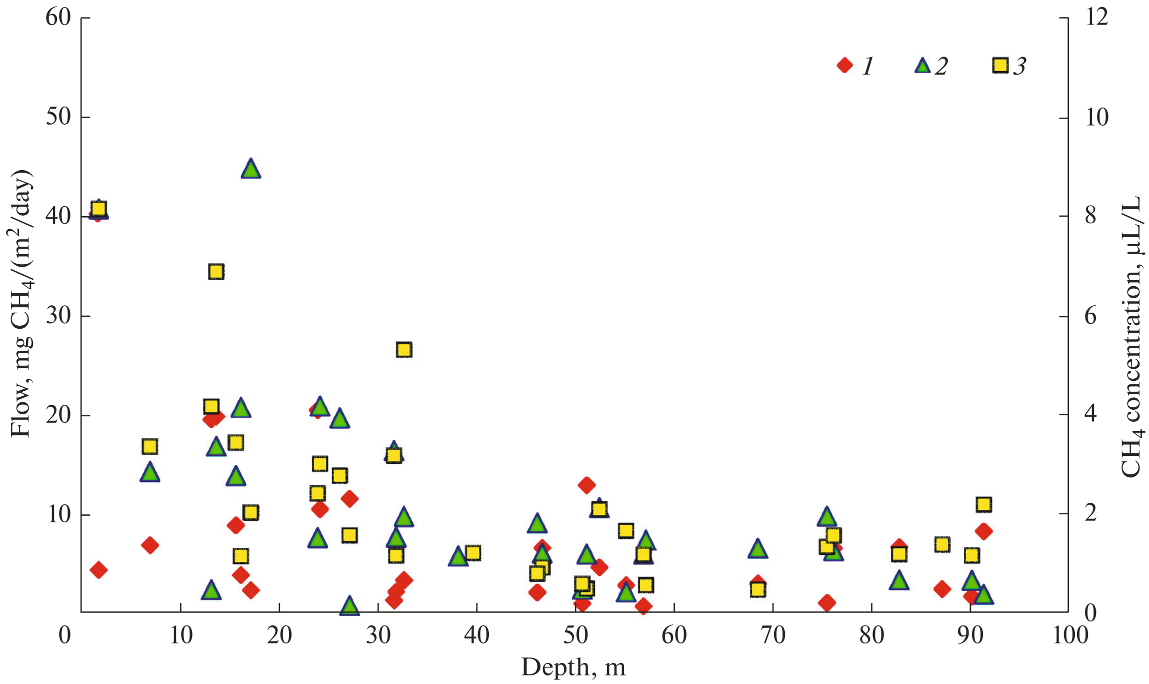

Fig. 5. Changes in the specific methane flux into the atmosphere and its concentrations in the Zeya Reservoir water with station depth during the warm period according to combined survey data in 2021 and 2022: (*1*) specific methane flux; (*2, 3*) respectively, methane content in the bottom and surface layers of water.

idle discharges due to low inflow. On the day of sampling in the hydroelectric power station upstream and downstream, the CH_4 content in the upstream and downstream was approximately the same at the level of 0.1–0.15 mg/m^3; this value is comparable to the accuracy of measuring the CH_4 concentration in water. The water flow through the turbines was 726 m^3/s. Thus, it is accepted that, during the period of work in 2022, there was no emission of CH_4 during the discharge of water through the dam into the downstream.

Water Area Zoning

There is a morphological zoning of the Zeya Reservoir, according to which the reservoir along its length is divided into eight regions (Shesterkin, 2015).

As part of this work, the authors identified seven areas in the Zeya Reservoir waters. These areas were identified by experts, based on materials from field work during the warm period of 2021 and 2022, as well as on the results of work carried out in March 2022 (Terskii et al., 2023). When carrying out zoning, the following indicators were taken into account: the predominance of expressed water mass (WM); spatial isolation; the presence of significant tributaries; and magnitude, range, and nature of changes in CH_4 content and fluxes identified during expeditions in 2021–2022. Characteristics of districts are given in Table 5, and the zoning scheme is given in Fig. 6.

Methane Emissions from the Surface of the Zeya Reservoir

Specific CH_4 flux values in the fall of 2021 (Table 6) were noticeably lower than in the summer of 2022 (Table 7). The CH_4 emission coefficient for the growing season was 8.6–11.1 kgCH_4 ha/year and 13.2–17.4 kgCH_4 ha/year in 2021 and 2022, respectively. The smallest contribution to CH_4 emission comes from the deep-sea, narrow dam part of the Canyon, and the largest is from the vast Large Sea, especially under conditions of a small influx of river water during the low-water warm period of 2022. Individual “hot spots,” despite their small area, can also make a significant contribution to total methane emissions. An assessment of this contribution very much depends on the way they are taken into account when calculating total emissions. For the lower estimate, the hot spots and shallow water stations were counted with the same weight as other stations within the area. For the upper estimate, the areas of shallow waters (up to 30 m) were calculated, which were used as weighting coefficients when taking into account shallow water stations within the regions.

DISCUSSIONS

In accordance with the work of (Edelshtein et al., 1984), three main water masses (WMs) were distinguished in the Zeya Reservoir in the warm period of the year: the Zeya River, the Gilyuy River, and the res-

Table 5. Characteristics of Zeya Reservoir areas

District number	District name	Characteristic
1	Canyon, dam part (below Gilyuy Bay)	Deepest part of the reservoir (up to 95 m). WM formation is caused by the connection of the reservoir and Gilyuy water masses. Wind mixing is much weaker than in the Large Sea. The shores are rocky
2	Canyon, upper part (above Gilyuy Bay)	Reservoir deepwater part (up to 86 m). Reservoir WM predominates. Wind mixing is much weaker than in the Large Sea. The shores are rocky
3	Gilyuy Bay	Bay in the Gilyuy River valley (depth up to 86 m). The Gilyuy WM stands out due to significant river inflow. Water has increased mineralization. Wind mixing is much weaker than in the Large Sea. In winter, the ice cover is not uniform everywhere—polynyas and caverns are observed
4	Large Sea	Relatively deepwater part of reservoir (depths from 30–40 to 50–60 m). Zeya River bed is practically not expressed under water. Wind mixing affects only the upper horizons; the depth of the temperature jump layer is not the same across the area. At depths below 30 m, winter reservoir WM predominates. Extensive drainage at low water levels in areas of abrasion-accumulative shores
5	Middle Sea	Relatively shallow part of reservoir (depths up to 30–35 m). Zeya River bed under water is weakly expressed. Wind mixing affects only the upper horizons
6	Shallow bays with large tributaries	Shallow water areas of reservoir (less than 20 m at NHL). Bays into which relatively large tributaries flow (Bryanta–Unakha–Utugai, Temna, Urkan, Mulmuga). In summer, there is increased mineralization at the bottom; the water temperature at the bottom is more than 5°C. Wind mixing affects a significant part of the water column. The banks are low and often swampy
7	Small Sea	Reservoir shallow part (depths up to 20 m), the channel is narrow, the old valley under water is well defined, in shallow waters tree trunks are above the water. Strong influence of lateral inflow and Zeya River on the temperature distribution, oxygen, and especially methane; surging disturbances of temperature stratification throughout the entire thickness. Influence of the Argi River is especially strong, expressed in increased concentrations of CH_4 throughout the entire thickness

ervoir in various seasonal modifications. River WMs were present mainly in the immediate vicinity of the mouths of the corresponding rivers. The Gilyuy WM was also found in the Canyon near the Gilyuy Bay. The reservoir itself was mainly filled with reservoir water in the following modifications: winter near-bottom, summer in the central region (we call this area the Large Sea), and summer in the lower region.

During the warm period of 2021 and 2022, we identified four WMs characteristic of the Zeya Reservoir in the first years after its filling (Edelshtein et al., 1984). The winter reservoir WM, located in the bottom layer of water in the Canyon and the Large Sea below 20–40 m, is characterized by relatively high mineralization (up to 45 mg/L), very low water temperature (about 4–6°C), and uniform oxygen content at the level 50–60% (which was typical for the winter of 2022, when the authors also carried out expeditionary research). The Gilyuy WM, adjacent to the Canyon lower part, in a layer of 10–25 m, is characterized by lower mineralization (about 25–30 mg/L) and increased oxygen content (up to 100–105% in the summer of 2022). The summer reservoir WM, located in the water column upper layer (up to 10–15 m from the surface), is common in the Canyon, in the Large and Middle Seas. The river WM, mainly the Zeya, fills mainly the reservoir upper reaches and the Small Sea. Not only Zeya River flow, but also the wind and other tributaries, lead to heterogeneity in the distribution of characteristics over depth.

Setup phenomena, wind-driven effects, as well as wind mixing, are a significant factor in the aeration of water at depths below the TJL and the CH_4 oxidation in the water of a wide part of the water area. In the Canyon, the influence of surge phenomena was not detected. Due to the high frequency of strong winds in the summer–autumn period, the temperature stratification nature of Zeya Reservoir is heterogeneous across the water area. Upwelling zones were identified during expeditionary observations in the Large Sea in 2021 and in the Small Sea in 2022. Most likely, the spatial heterogeneity in the Large Sea is generally characteristic of autumn. It is possible that the drift of surface WM and upwelling of bottom WM is one of the main mechanisms for mixing bottom water in the Zeya

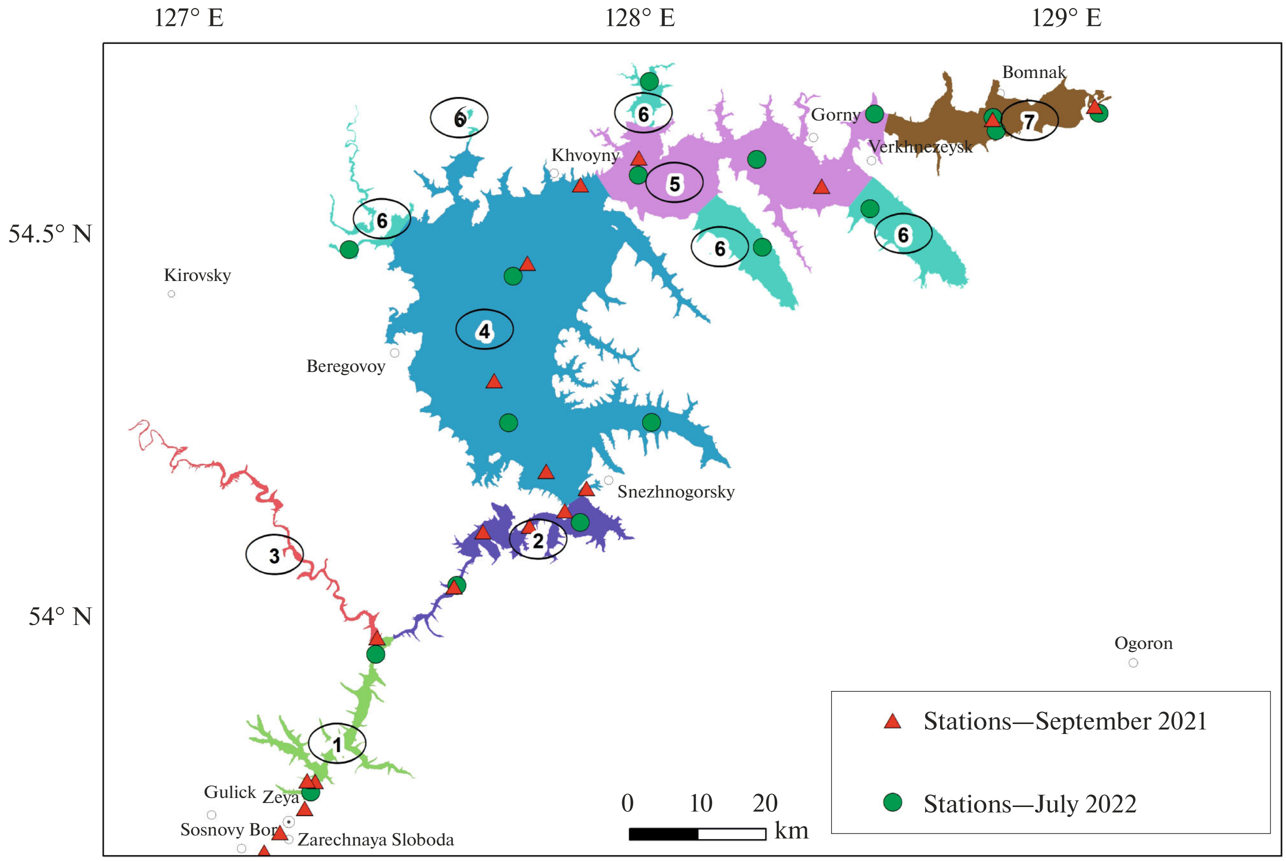

Fig. 6. Zoning scheme for the Zeya Reservoir water area (numbering and names of districts correspond to Table 5).

Table 6. Total emission and emission coefficient of CH_4 from the surface of the Zeya Reservoir in autumn 2021

District	District number (see Fig. 6)	September 17–23, 2021				
		district area, km^2	average (specific) flux, $mgCH_4/m^2/day$	range of measured fluxs, $mgCH_4/m^2/day$	total methane emission, tCH_4/day	emission factor, $kgCH_4$ ha/year (135 days)
Canyon dam part	1	73.4	3.3	2.1–5.2	0.2	4.4
Upper Canyon	2	115.5	2.2–45*	0.1–246*	0.2–5.2	2.8–62
Gilyuy Bay	3	36.8	2.3	0.7–3.9	0.1	3.1
Large Sea	4	1296	3.9	0.7–4.6	5.1	5.3
Middle Sea	5	444	4.8	1.8–9.8	2.1	6.4
Bays	6	437	6.5–13	3.2–29	2.8–5.7	8.8–17
Small Sea	7	218	11–26	0.7–56	2.5–5.6	15–35
Hot spot (3–5% of area 2)	–	–	138	30.5–246	0.48–0.8	–
Dam release	–	–	–	–	0.175	–
ENTIRE RESERVOIR		**2621**	**6.4–8.3**	**0.7–246**	**16.7–21.7**	**8.6 –11.1**

* Upper limit of the range of measured and average specific flux for a given area is indicated for a scenario in which the hot spot is taken into account as one of the stations in the area.

Table 7. Total emission and emission coefficient of CH_4 from the surface of Zeya Reservoir in the summer of 2022

District	District number (see Fig. 6)	July 26–31, 2022				
		district area, km^2	average (specific) flux, $mgCH_4/m_2/day$	range of measured fluxs, $mgCH_4/m_2/day$	total methane emission, tCH_4/day	emission factor, $kgCH_4$ ha/year (135 days)
Canyon dam part	1	63.4	7.4–9.8	7.2–12	0.5–0.6	10–13
Upper Canyon	2	106	4.6–6.1	3.6–9.3	0.5–0.6	6.1–8.2
Gilyuy Bay	3	30.7	8.7	7.2–10.2	0.3	12
Large Sea	4	1213	6.2–9.1	1.2–28.7	7.5–11	8.4–12
Middle Sea	5	408	7.9–9	2.5–19.6	3.2–3.7	11–12
Bays	6	315	27–35	2.2–137	8.4–11	36–48
Small Sea	7	151	13–16	2.9–42	2.0–2.4	18–22
Dam release	–	–	–	–	0	–
ENTIRE RESERVOIR		**2287**	**9.8–13**	**1.2–137**	**22.4–29.8**	**13.2–17.4**

Reservoir. Despite the fact that upwelling is a phenomenon that is more characteristic of seas and oceans, it is also common for large lakes and reservoirs (*Ekosistema Onezhskogo ozera*..., 1990).

During field work in 2022, after a night of heavy rain, a stream (hereinafter referred to as the Zimovye stream) was discovered on the shore, flowing from the swamp massif and into the Small Sea of Zeya Reservoir. Presumably, the stream flows along the roof of permafrost. The water temperature in the stream was 6.0°C. Its chemical composition was characterized by very high color, iron and organic matter content, lower pH, and low mineralization, but very high organic carbon (OC) content. Slope runoff from swamps on permafrost apparently does not itself bring CH_4 into the reservoir, but can bring a large amount of organic matter, which, when deposited, contributes to the production of CH_4 in bottom sediments. The hypothesis of the permafrost origin of the Zimovye stream is also supported by information about melted permafrost waters given in literary sources. Thus, expeditionary research in 2020 in the Bureya River upper reaches (Tashiro et al., 2020) showed that, during the snowmelt season, large amounts of dissolved OC are formed in waterlogged surface soils along with dissolved iron (Fe), leading to the significant transport of Fe and OC. Summer rains not only increase Fe and OC concentrations in rivers, but also promote the accumulation of Fe in soils on permafrost within wetlands. In the examined stream, the CH_4 content in the water was very low—0.09 μL/L.

CH_4 release during water discharge into the tailwater can make a large contribution to the total release of CH_4 into the atmosphere from reservoirs. According to studies of Amazonian reservoirs, about 70% of CH_4 diffuses into the atmosphere when water is released through a dam into the tailwater (Kemenes, 2016). At the Zeyskaya HPP dam, in the absence of operation through surface spillways in 2022, no CH_4 emissions into the atmosphere were detected, and in the fall of 2021, when water was discharged through the dam into the downstream, methane emissions into the atmosphere amounted to 175 $kgCH_4/day$, or 0.09% of total CH_4 emissions during the warm period. At the same time, in the winter of 2022, the flow amounted to 27.4 $kgCH_4/day$, even in the absence of surface spillways (Terskii et al., 2023), and, apparently, was the only source of CH_4 emissions during the freeze-up period.

The main autochthonous source of CH_4 in the Zeya Reservoir is bottom sediments of the water area shallow part, since there is a pattern of decreasing methane flows from the shores to the reservoir center. Shallow-water bays, the bottom of which is covered with regularly supplied woody material from the shores (this conclusion was made from the presence of organic suspended matter and woody residues at the bottom of such bays), are common in certain areas of a coastline, and, apparently, are not an area source of CH_4, but rather pointwise on the scale of the entire reservoir. Despite the increased fluxes of CH_4 in such bays by several orders of magnitude, its concentrations in water near the shores are only a few microliters per liter higher than the background ones.

The main allochthonous source of CH_4 is the Argi River—a large swamp tributary of the reservoir in its upper reaches. As a result of all expeditionary research, including winter work in March 2022 (Terskii et al., 2023), it was revealed that the Argi River is one of the large tributaries of Zeya Reservoir, which drains a vast swamp area, and is a significant source of CH_4 and organic matter entering the reservoir. This is a relatively large river (F = 7090 km^2, L = 350 km), comparable to the Zeya itself, and accounting for approximately 9% of the entire catchment area of Zeya Reservoir in the upper reaches. Argi River water, when it flows into the reservoir, is saturated with hydrogen sulfide and CH_4, and it has high mineralization and color and low silicon and oxygen content.

Estimates of specific CH_4 fluxes (0.1–56 mgCH_4/m^{2}day), obtained by the authors during the expeditionary studies described in this article in the Zeya Reservoir, are generally consistent with global data. In (Varis et al., 2012) for reservoirs in the boreal zone, the CH_4 emission range is 1–100 mgCH_4/m^{2}day. In the Zeya Reservoir, the authors identified zones with both very low CH_4 flows and individual "hot spots" with flow values exceeding the upper limit of this estimate. CH_4 emission factors from the Zeya Reservoir in 2021 and 2022 (8.6–17.4 kgCH_4/ha) correspond to the coefficients presented in the amendments to the 2019 IPCC guidelines, which were formed more than 20 years ago (https://www.ipcc.ch/report/2019-refinement-to-the-2006-ipcc-guidelines-for-national-greenhouse-gas-inventories). The coefficient presented by the IPCC 2019 for reservoirs in the boreal zone is 13.6 kgCH_4/ha (with a 95% confidence interval of the mean value of 7.3–19.9 kgCH_4/ha).

CONCLUSIONS

As part of this study, for the first time in the Zeya Reservoir, in situ measurements of CH_4 concentration in water and its specific fluxes from the water surface were carried out, together with hydrological and hydrochemical surveys during the warm periods of the relatively high-water year 2021 and the low-water year 2022. Compared to September 2021, in July 2022, the heat reserve in the Zeya Reservoir was significantly lower, despite the higher temperature of the water surface layer. Mineralization was higher, and the oxygen content on average was almost the same.

The CH_4 content in water and its specific fluxes decrease from the shores and bays to the reservoir center. Apparently, the main sources of organic matter and methane are swampy tributaries, as well as coastal areas of the water area, where organic matter flows from the shores. The CH_4 total emission from the surface of Zeya Reservoir is significantly higher in the summer of 2022, when the maximum heating of shallow waters is observed, even despite the smaller water area than in the fall of 2021. According to the authors' estimates, the total emission of CH_4 from the water surface of Zeya Reservoir in the autumn of 2021 amounted to 16.7–21.7 tCH_4/day; in the summer of 2022 it was 22.4–29.8 tCH_4/day.

Methane release during the water evacuation through the structures of the hydroelectric complex in the warm period is associated with the operating mode of surface spillways. In the absence of surface spillway operation in the summer of 2022, no methane emissions occurred. In the fall of 2021, despite the presence of a surface spillway, the emission of CH_4 was insignificant (0.175 tCH_4/day), accounting for about 0.09% of its total emission from the water surface of Zeya Reservoir.

ABBREVIATIONS AND NOTATION

DEM	Digital elevation model
GHGs	Greenhouse gases
NHL	Normal headwater level
TJL	Temperature jump layer
WM	Water mass
WL	Water level
OC	Organic carbon

FUNDING

This work was supported by ongoing institutional funding. No additional grants to carry out or direct this particular research were obtained.

CONFLICT OF INTEREST

The authors of this work declare that they have no conflicts of interest.

REFERENCES

Alekin, O.A., *Osnovy gidrokhimii* (Fundamentals of Hydrochemistry), Leningrad: Gidrometeoizdat, 1970.

Arefina, T.I., Boroditskaya, G.V., Bul'on, V.V., et al., *Gidroekologicheskii monitoring zony vliyaniya Zeiskogo gidrouzla* (Hydroecological Monitoring of the Influence Zone of the Zeya Hydroelectric Complex), Khabarovsk: DVO RAN, 2010.

Bastviken, D., Santoro, A.L., Marotta, H., Pinho, L.Q., Calheiros, D.F., and Crill, P., Methane emissions from Pantanal, South America, during the low water season: Toward more comprehensive sampling, *Environ. Sci. Technol.*, 2010, vol. 44, no. 14, pp. 5450–5455.

Darling, W.G. and Gooddy, D.C., The hydrogeochemistry of methane: Evidence from English groundwaters, *Chem. Geol.*, 2006, vol. 229, no. 4, pp. 293–312.

Deemer, B.R. and Holgerson, M.A., Drivers of methane flux differ between lakes and reservoirs, complicating global upscaling efforts, *J. Geophys. Res.: Biogeosci.*, 2021, vol. 126, no. 4, p. e2019JG005600.

Deemer, B.R., Harrison, J.A., Li, S., Beaulieu, J.J., DelSontro, T., Barros, N., Bezerra-Neto, J.F., Powers, S.M., Dos Santos, M.A., and Vonk, J.A., Greenhouse gas emissions from reservoir water surfaces: A new global synthesis, *BioScience*, 2016, vol. 66, no. 11, pp. 949–964.

Edel'shtein, K.K., Ershova, M.G., and Nemal'tsev, A.S., Hydrological features of the Zeya reservoir during its filling, in *Gidrologiya Baikala i drugikh vodoemov* (Hydrology of Lake Baikal and Other Water Bodies), Novosibirsk: Nauka, 1984, pp. 146–156.

Ekosistema Onezhskogo ozera i tendentsii ee izmeneniya (The Ecosystem of Lake Onega and Trends in Its Change), Leningrad: Nauka, 1990.

Elistratov, V.V., Maslikov, V.I., Sidorenko, G.I., and Molodtsov, D.V., Greenhouse gas emissions from hydroelectric power station reservoirs: analysis of research experience and organization of experiments in Russia, *Al'tern. Energ. Ekol.*, 2014, no. 11, pp. 146–159.

Gar'kusha, D.N. and Fedorov, Yu.A., *Faktory formirovaniya kontsentratsii metana v vodnykh ekosistemakh* (Factors in the Formation of Methane Concentrations in Aquatic Ecosystems), Taganrog: Izd. Yuzhn. fed. univ., 2021.

Grechushnikova, M.G., Repina, I.A., Stepanenko, V.M., Kazantsev, V.S., Artamonov, A.Yu., Varentsov, M.I., Lomova, D.V., Mol'kov, A.A., and Kapustin, I.A., Spatiotemporal changes in methane content and emission in reservoirs with different water exchange coefficients, *Izv. Russ. Geogr. O-va*, 2018, vol. 150, no. 5, pp. 14–33.

Grechushnikova, M.G., Repina, I.A., Stepanenko, V.M., Kazantsev, V.S., Artamonov, A.Yu., and Lomov, V.A., Methane emission from the surface of the Mozhaisk valley-type reservoir, *Water Resour.*, 2019, vol. 40, no. 3, pp. 247–255. http://aisori-m.meteo.ru/. http://oopt.info/zevsky/phvsgeo.html. http://www.rushydro.ru/. https://www.ipcc.ch/report/2019-refinement-to-the-2006-ipcc-guidelines-for-national-greenhouse-gas-inventories/.

Kemenes, A., Melack, J., and Forsberg, B., Downstream emissions of CH_4 and CO_2 from hydroelectric reservoirs (Tucurui, Samuel, and Curua-Una) in the Amazon basin, *Inland Waters*, 2016, vol. 6, pp. 1–8.

Regulatory document. Mass concentration of methane and carbon dioxide in the atmospheric surface layer. Methodology of measurements using RD 52.44.816-2015 gas chromatography.

Regulatory document. Federal list of measurement techniques approved for the monitoring of environmental pollution RD 52.18.595–96 (as amended by Change no. 1, approved by Roshydromet on October 11, 2002, and Change no. 2, approved by Roshydromet on October 28, 2009).

Repina, I.A., Terskii, P.N., Gorin, S.L., Agafonova, S.A., Akhmerova, N.D., Vasilenko, A.N., Grechushnikova, M.G., Grigor'ev, V.Yu., Kazantsev, V.S., Lisina, A.A., Lomov, V.A., Mishin, D.V., Sazonov, A.A., Stepanenko, V.M., Sokolov, D.I., et al, Field measurements of methane emission at largest reservoirs in Russia in 2021. The start of large-scale studies, *Water Resour.*, 2022, vol. 49, no. 6, pp. 1003–1008.

Rules for the use of water resources of the Zeya reservoir on Zeya River (approved by order of the Federal Agency for Water Resources of July 18, 2018 no. 151) 2018.

Shesterkin, V.P., Salt composition of Zeya Reservoir waters, *Vodn. Khoz. Ross.: Probl., Tekhnol., Upr.*, 2015, no. 5, pp. 32–42.

Shesterkin, V.P., Sirotskii, S.E., and Shesterkina, N.M., Microelements in Zeya Reservoir waters, in *Zhizn' presnykh vod* (Life in Freshwater), Vladivostok: BPI DVO RAN, 2016, pp. 47–53.

Skhema kompleksnogo ispol'zovaniya i okhrany vodnykh ob"ektov po basseinu reki Amur (rossiiskaya chast'). Proekt. Kniga 1 (Scheme for the Integrated Use and Protection of Water Bodies in the Amur River Basin (the Russian Part. Project. Book 1), Vladivostok: Dal'NIIVKh, 2010.

Tashiro, Y., Yoh, M., Shiraiwa, T., Onishi, T., Shesterkin, V., and Kim, V., Seasonal variations of dissolved iron concentration in active layer and rivers in permafrost areas, Russian Far East, *Water*, 2020, vol. 12, no. 9, p. 2579.

Terskii, P.N., Gorin, S.L., Grechushnikova, M.G., Agafonova, S.A., and Repina, I.A., Hydrological conditions of methane emission from the Zeya reservoir in the warm and cold periods of 2021–2022, in *GREG 2022: Mezhdunarodnaya nauchno-issledovatel'skaya konferentsiya "Emissiya parnikovykh gazov segodnya i v geologicheskom proshlom: istochniki, vliyanie na klimat i okruzhayushchuyu sredu". Sbornik tezisov* (GREG 2022: International Research Conference "Greenhouse Gas Emissions Today and in the Geological Past: Sources and Impact on Climate and Environment": Collection of Abstracts), Kazan: Kazan. fed. univ., 2023, p. 46.

Varis, O., Kummu, M., Härkönen, S., and Huttunen, J.T., Greenhouse gas emissions from reservoirs, in *Impacts of Large Dams: A Global Assessment*, Berlin: Springer, 2011, pp. 69–94.

Wing, S.R., Bowman, M.H., Smith, F., and Rutger, S.M., Analysis of biodiversity patterns and management decision making processes to support stewardship of marine resources and biodiversity in Fiordland: A case study, Report, Ministry for the Environment, Wellington, New Zealand, 2004.

Translated by V. Selikhanovich